Analysis of burner operation inside an Enclosed Ground Flare

Joseph Smith[¥], Russell M. Keckler[£], Ahti Suo-Anttila[§], Zach Smith[⸸], Vikram Sreedharan[⸸]

[¥]*Chemical and Biochemical Engineering, Missouri Univ of Sci and Tech, Rolla, MO 65409 USA*
[£]*APTIM | LFG Specialties, Findly, Ohio, USA*
[§]*Computational Engineering Analysis LLC, 4729 Paso Del Puma Ne, Albuquerque, NM 87111 USA*
[⸸]*Elevated Analytics Consulting, 343 East 4th Street, Suite 104, Rexburg, ID 83440 USA*

Abstract

An industrial enclosed ground flare used as part of a large refinery project has been analyzed to assess combustion stability and performance under low and high flow conditions. This flare includes a large combustion chamber directly above the burner deck with Low Flow (LF) burners that fire up to 9 MMBtu/hr plus High Flow (HF) burners designed to fire at 8 to 45 MMBtu/hr. The LF burners operate with simple "diffusion" flames while the HF burners use "pre-mixed" flames designed to limit NOx emissions. During initial commissioning tests, the flare was operated over a range of process conditions. Testing results indicated the following:

1. Relative flow velocity through the burner throat was critical to maintaining a stable flame above the burner,
2. Burner placement inside the flare impacted flow profiles that led to asymmetric flow and produced low pressure fluctuations during normal operations, and
3. High frequency pressure fluctuations observed near the burner were attenuated and became low frequency fluctuations at the stack exit.

This paper describes results of the CFD analysis of this enclosed flare that focused on flame stability and noise generation inside the flare during operation.

Key Words: Thermo-Acoustic Coupling, Enclosed Flare, LES CFD Model, Noise, Premixed Burner

INTRODUCTION

Thermoacoustic vibrations in process equipment represents a coupling between the temperature gradients and flow profiles in the combustion chamber and the natural sound frequency of the chamber. Earlies work has examined thermo-acoustic coupling observed in a heated tube closed at one end with the other end open and a heat source included in the closed end. This configuration, referred to as a Sondhauss tube, is named after the individual who originally studied and reported this phenomenon [1]. When the heat source is hot enough, a loud sound is created by the coupling between the volume expansion in the air caused by the heat source and the natural sound frequency of the tube. This phenomena has also been observed in gas turbines [2], [3], [4] and in process equipment where burners are installed at the closed end of a combustion chamber which is open to the atmosphere such as in process heaters and sulfur furnaces

Over the years, various approaches have been taken to analyze thermos-acoustic coupling including "*Lumped parameter*" models [5], "*Acoustic Element Network*" models [6] and more recently "*Transient CFD*" models employing refined grids with complex physical sub-models for turbulence and chemical kinetics to capture the thermo-acoustic coupling inside a reactor [7].

Of these approaches, transient CFD models using chemical reaction sub-models coupled to turbulent mixing sub-models have been most successful in simulating the coupling between flame heat release and natural acoustic modes in a combustion chamber. In the present work, we used an "Large-Eddy Simulation" (LES) based CFD code called C3d. [8] This code has been previous used to analyze other transient phenomena such as flare ignition and unsteady burner operation [9], [10], [11].

This paper reports on work using this transient CFD code to simulate thermos-acoustic coupling in an enclosed gas flare (see Figure 1) installed at an LNG facility.
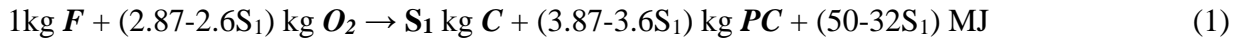
TRANSIENT CFD COMBUSTION MODELING

The CFD tool used in this work, C3d, links turbulent reaction chemistry with radiative transport, as described elsewhere [12], to simulate the thermos-acoustic coupling inside an enclosed ground flare.   This code has been validated and verified by comparing code predictions to measured results from several lab scale and pilot scale experiments [13] and has been shown to provide "reasonably" accurate estimates for this type of reacting flow system. For transient combustion analysis, Large Eddy Simulation (LES) is better than other approaches (i.e., Reynolds Averaged Navier-Stokes or RANS) to capture flow structure important in this application. C3d has also been used to analyze Multi-Point Ground Flares (MPGFs), elevated air- and steam-assisted flares, and utility flares with detailed kinetics to describe flare performance [10], [14]. C3d predicts flame size and shape, and associated radiation flux from flames with validation by direct comparison of radiation predictions and measurements taken

during single-burner and multi-burner flare tests conducted under no-wind and low-wind conditions [11].

Figure 1 - Enclosed Flare Chamber and Stack with burner orientation

Figure 2- Plan view of Burner layout inside the Enclosed Ground Flare

MODELING METHODOLOGY

To model thermos-acoustic coupling, the transient, LES based CFD code C3d has been used. Initially, this code was developed to simulate the combustion process occurring in large pool fires [13] but more recently has also been applied to study wind effects on multi-point ground flares [14], transient ignition of elevated multi-point flares [11], and safety issues related to radiation from adjacent ground flares [10]. This code has also previously been used to analyze thermo-acoustic coupling in process heaters and waste incinerators [15], [16].

C3d is well suited to investigate the transient coupling between turbulent reacting flow and the natural acoustic behavior of a combustion device because it describes the turbulent fluid mixing of fuel and oxidizer with transient chemical reactions. C3d uses the general global reaction mechanism shown below:
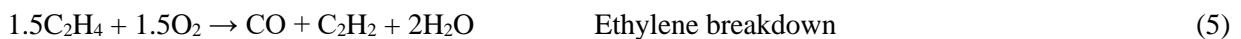
$$1\text{kg } \boldsymbol{F} + (2.87\text{-}2.6S_1) \text{ kg } \boldsymbol{O_2} \rightarrow \boldsymbol{S_1} \text{ kg } \boldsymbol{C} + (3.87\text{-}3.6S_1) \text{ kg } \boldsymbol{PC} + (50\text{-}32S_1) \text{ MJ} \tag{1}$$

$$1\text{kg } \boldsymbol{F} + 0.3 \text{ MJ} \rightarrow S_2 \text{ kg } \boldsymbol{C} + (1\text{-}S_2) \text{ kg } \boldsymbol{IS} \tag{2}$$

$$1\text{kg } \boldsymbol{C} + 2.6 \text{ kg } \boldsymbol{O_2} \rightarrow 3.6 \text{ kg } \boldsymbol{CO_2} + 32 \text{ MJ} \tag{3}$$

$$1\text{kg } IS + (2.87 - 2.6S_2)/(1\text{-}S_2) \text{ kg } \boldsymbol{O_2} \rightarrow$$
$$(3.87 - 3.6S_2)/(1\text{-}S_2) \text{ kg } \boldsymbol{PC} + (50\text{-}32S_2)/(1\text{-}S_2) \text{ MJ} \tag{4}$$

where first reaction (Eq. 1) describes the incomplete combustion of hydrocarbon fuel ($\boldsymbol{F}$) with oxygen to produce products of combustion ($\boldsymbol{PC}$) and soot ($\boldsymbol{C}$). This reaction produces S_1 kilograms of soot per kilogram of fuel consumed where S_1 depends on the fuel (0.005 found appropriate for light hydrocarbons [17]). Reaction 2 (Eq. 2) describes endothermic fuel cracking to produce S_2 kilograms of soot (0.15 found appropriate for light hydrocarbons). Reaction 3 (Eq. 3) consumes soot and oxygen to produce carbon dioxide and some energy. Reaction 4 (Eq. 4) consumes the Intermediate Species ($\boldsymbol{IS}$) formed in the second reaction with additional oxygen to form more products of combustion ($\boldsymbol{PC}$) and energy. These reactions are approximated using the Eddy-Dissipation Concept method originally developed by Magnussen and Hjertager [18] and elsewhere by Smith, et al., [14]. This simplified combustion model includes 6 species which have been found adequate for most combustion simulations.

GENERAL COMBUSTION MODEL

For systems burning complex mixtures of hydrocarbons, a "modified" combustion model covering a wide range of fuels and intermediate species be used [19]. To use this model, fuel combustion is separated into primary fuel breakdown forming intermediate species followed by combustion of those intermediate species.

Primary fuel breakdown reactions are shown below (Eq. 5 – Eq. 12) for wide range of fuels:

$$1.5C_2H_4 + 1.5O_2 \rightarrow CO + C_2H_2 + 2H_2O \qquad \text{Ethylene breakdown} \tag{5}$$

$$C_3H_8 + 1.5O_2 \rightarrow C_2H_2 + 2H_2O + CO + H_2 \qquad \text{Propane breakdown} \tag{6}$$

$$C_2H_6 + 0.5O_2 \rightarrow 0.5C_2H_2 + CO + H_2 \qquad \text{Ethane breakdown} \qquad (7)$$

$$C_3H_4 + O_2 \rightarrow C_2H_2 + H_2O + CO \qquad \text{Propadiene breakdown} \qquad (8)$$

$$C_5H_{12} + 4O_2 \rightarrow C_2H_2 + 5H_2O + 3CO \qquad \text{N-Pentane breakdown} \qquad (9)$$

$$C_4H_6 + 4O_2 \rightarrow 2C_2H_2 + H_2O \qquad \text{1,2, Butadiene breakdown} \qquad (10)$$

$$C_3H_6 + 1.5O_2 \rightarrow C_2H_2 + 2\,H_2O + CO \qquad \text{Propylene breakdown} \qquad (11)$$

$$C_{12}H_{26} + 6.5O_2 \rightarrow 7H_2O + 2CH_4 + 2C_2H_2 + 6CO \quad \text{Dodecane breakdown} \qquad (12)$$

These reactions can be used individually or combined into a single fuel breakdown reaction for a gas mixture by applying the respective mole fractions of each component and adding the mole fraction weighted reactions terms together to form a single fuel breakdown reaction for the mixed fuel. For example, combustion of a flare gas mixture of ethylene, propane and propylene could be approximated by combing the individual fuel breakdown reactions for ethylene (Eq. 5), propane (Eq. 6) and propylene (Eq. 11) using the mole fractions of each specie in the gas mixture.

Even more complex hydrocarbons, not listed above, could be approximated by breaking down the hydrocarbon into CO, C_2H_2, H_2 and H_2O with stoichiometric coefficients estimated using three simple rules:

1. Heavy sooting hydrocarbons produce more C_2H_2 and possibly a small amount of soot,
2. The heat release for primary fuel breakdown should be adjusted by producing more H_2O for higher heat release or more H_2 for less heat release, and
3. The oxygen consumption balance, and associated CO production should be determined by an elemental balance.
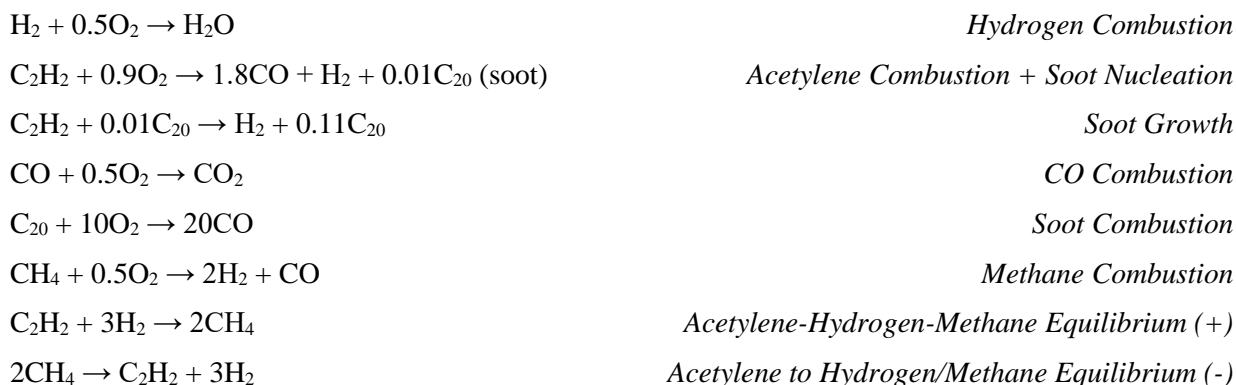
Testing this approach has shown that the combustion model based on methane combustion has mild sensitivity to the primary breakdown reactions, which allows the user flexibility in developing advanced combustion models for mixed fuels. Testing also shows that secondary reactions are mostly determined by the flame temperature and soot production.

For the present flare, flare gas was composed mainly of methane and carbon dioxide (see Figure 3). With this composition, the combustion model was formed and used in the analyses.

Component	Gross Heating Value	Net Heating Value	Gas Composition
	Btu/scf	Btu/scf	Mol%
Nitrogen (N2)	0	0	0.053
Carbon dioxide (CO2)	0	0	48.460
Water (H2O)	0	0	5.334
Methane (CH4)	1012	911	18.402
Ethane (C2)	1783	1631	9.846
Ethylene (C2=)	1600	1499	0.084
Propane (C3)	2557	2353	9.735
n-Butane (C4)	3369	3101	6.389
iso-Pentane (i-C5)	4001	3698	1.408
Hexane Plus	5222	4971	0.259
Hydrogen Sulfide (H2S)	637	587	0.030
		Total Gas Composition	100.000
		Gross Heating Value (High Heating Value)	897.35
		Net Heating Value (Lower Heating Value)	822

Figure 3 - Flare gas composition considered in this work

The secondary reactions used in these simulations have been calibrated against test data and found not to change from simulation to simulation and are also grid independent.

$H_2 + 0.5O_2 \rightarrow H_2O$ *Hydrogen Combustion*

$C_2H_2 + 0.9O_2 \rightarrow 1.8CO + H_2 + 0.01C_{20}$ (soot) *Acetylene Combustion + Soot Nucleation*

$C_2H_2 + 0.01C_{20} \rightarrow H_2 + 0.11C_{20}$ *Soot Growth*

$CO + 0.5O_2 \rightarrow CO_2$ *CO Combustion*

$C_{20} + 10O_2 \rightarrow 20CO$ *Soot Combustion*

$CH_4 + 0.5O_2 \rightarrow 2H_2 + CO$ *Methane Combustion*

$C_2H_2 + 3H_2 \rightarrow 2CH_4$ *Acetylene-Hydrogen-Methane Equilibrium (+)*

$2CH_4 \rightarrow C_2H_2 + 3H_2$ *Acetylene to Hydrogen/Methane Equilibrium (-)*

For conditions where low oxygen and high temperature exist, hydrocarbon and soot reforming reactions also occur. Normal combustion chemistry is known to generate H^+ and OH^- radicals from primary fuel breakdown reactions. In this combustion model, these radicals are modeled as water vapor (H_2O) since water vapor is considered an oxidizing agent. This means water vapor can react with the primary fuel to produce C_2H_2, CO, and H_2. It can also oxidize soot to produce CO and H_2. Thus, for example, the reforming reactions for ethylene are:

$C_2H_4 + H_2O \rightarrow CO + 0.5C_2H_2 + 0.5H_2$ *Ethylene – Water Reforming*

$C_{20} + 20H_2O \rightarrow 20CO + 20H_2$ *Soot – Water Reforming*

Global Arrhenius rate data used for the combustion model reactions include the primary reactants f_1 and f_2, the effective activation temperature T_A, the pre-exponential coefficient C, the global exponent p, and the temperature exponent B. Data used for the combustion model used in these analyses are presented in Table 1. Values listed here were derived from published values or by direct comparison to previous experimental work.

All kinetic reactions listed obey the global Arrhenius reaction equation. CO oxidation also includes the square root of water mole fraction weighting factor developed by Westbrook and Dryer [20]. Soot oxidation occurs at high temperature which makes the reaction chemistry boundary layer diffusion limited since soot is a particle with a boundary layer instead of a flammable gas. Thus, the temperature dependence of soot oxidation is controlled by the variation of mass transfer coefficient which is directly related to local temperature. Since soot oxidation in the water reforming reactions occurs faster than soot oxidation by oxygen, soot oxidation by oxygen is combined with the eddy breakup time delay since oxygen must diffuse into the flame zone from the surrounding atmosphere.

The enclosed ground flare considered in this work uses "Low-NOx" pre-mixed burners for firing rates above 9 MMBtu/hr and "low flow" diffusion burners for firing rates below 9 MMBtu/hr (see Figure 2). Low flow conditions are normal during flare startup, shut down and

low firing conditions. Since this flare processes gas from various parts of the plant, the flare operates over a wide range of firing conditions. Specific firing conditions considered in this analysis are listed in Table 2. Since the flare includes diffusion-based combustion in the low-flow burners and "pre-mixed" combustion in the high-flow burners, the transient simulation must be able to accurately represent both types of combustion. Thus, the LES based CFD code C3d is best suited to analyze this flare system.

Table 1- Arrhenius Reaction Coefficients for the general combustion model used in C3d for a Hydrocarbon Fuel

Reaction	f_1	f_2	$T_{A\,(K)}$	C (1/s)	B
Primary Fuel Breakdown (ethylene)	$[C_2H_4]^{0.1}$	$[O_2]^{1.65}$	0 K	1	2
Hydrogen Combustion	$[H_2]^{0.33}$	O_2	10000 K	1e8	0
Acetylene combustion & soot nucleation	$[C_2H_2]^{0.33}$	O_2	15110 K	2e8	2
Acetylene + soot growth	$[C_{20}]^{0.33}$	C_2H_2	15110 K	1e7	0
CO – Oxygen combustion	CO	$[O_2]^{0.25}[H_2O]^{0.5}$	20142 K	1e18	0
Soot combustion	$[C_{20}]^{0.33}$	O_2	0 K	0.5	0.75
Methane combustion	CH_4	O_2	15000 K	1e12	0
Forward Acetylene – Hydrogen – Methane	C_2H_2	H_2	15110 K	5e7	0
Reverse Acetylene – Hydrogen - Methane	CH_4	CH_4	23500 K	4e9	0
Ethylene - Water Reforming	C_2H_4	H_2O	15000 K	5e6	0
Soot – Water Reforming	$[C_{20}]^{0.1}$	$[H_2O]^{1.7}$	0 K	1.0	0.75

ANALYSIS OF ENCLOSED GROUND FLARE

The enclosed ground flare's main objective in the present application is to protect the environment by efficiently and cleanly combusting waste gas from the plant. During its commissioning tests, the enclosed flare was optimized to accomplish this purpose.

During initial testing, unstable combustion was observed during the transition between low-firing rate and high-firing rate conditions. Specifically, flame flashback in the premixed burners was observed plus flame pulsing in the diffusion burners was observed. These unsteady operations were also accompanied by high pressure spikes inside the flare which damaged the premixed burner.

Table 2 – Firing Scenarios considered during the analysis

CASE	Heat Release MMBTU/hr {LHV Basis}			
	Warm Low Fire	Warm High Fire	Cold Low Fire	Cold High Fire
CFD1	-	34	-	45
CFD2	-	34	-	23
CFD3	-	34	-	8
CFD4	-	17	-	45
CFD5	-	17	-	23
CFD6	-	17	-	8
CFD7	-	8	-	45
CFD8		8		23
CFD9		8		8
CFD10	2.5	-	-	45
CFD11	-	31.68	3.8	
CFD12	0.83	-		32.72

It was hypothesized that the high-pressure (high noise) levels in the flare at this firing rate was related to the relative flow velocity and flame speed at this condition. This hypothesis was supported by the observation of flame flash back in the premixed burners. The observation of unstable combustion above the diffusion flames were also thought to be related to flame speed and flow velocity.

To improve flare operation, the C3d code was used to analyze combustion inside the enclosed flare for the firing scenarios listed in Table 2. Twelve different CFD cases were completed with results analyzed for each firing condition. The original flare and burner designs were modified based on the CFD results. Design changes included changing the burner diffuser, setting the optimum flame tube height, and developing burner registers for the low-firing rate diffusion burners. Results of this work are presented below.

Diffuser Design Optimization

During pre-commissioning field tests, the flame was observed to become unstable and flash below the pre-mixed burner "diffuser" (see

Figure 4). This condition was observed at a medium firing duty where a stable premixed flame initially anchored to the flame holder began to oscillate inside the burner and flash back into the venturi premixing tube below the burner. For this burner design, the flame holder is intended to stabilize the premixed flame above the burner. After examination, it was determined the flame speed through burner was less than the flame speed which allowed flashback. This condition was modeled using CFD to investigate the relationship between burner design and flame speed. The initial CFD analysis considered the existing burner design which showed the flame flashback into the venturi tube as observed (see left image in **Error! Reference source not found.**). This CFD analysis confirmed field observations of the flame behavior for the initial burner design. CFD was then used to examine a burner which produced a higher flow velocity

through the burner. This analysis showed a stable flame above the burner (see right image in Figure 5). Since this CFD code examines transient behavior, this analysis was able to help optimize the burner design based on field observations and confirm the best design to ensure stable operation for all firing rates.
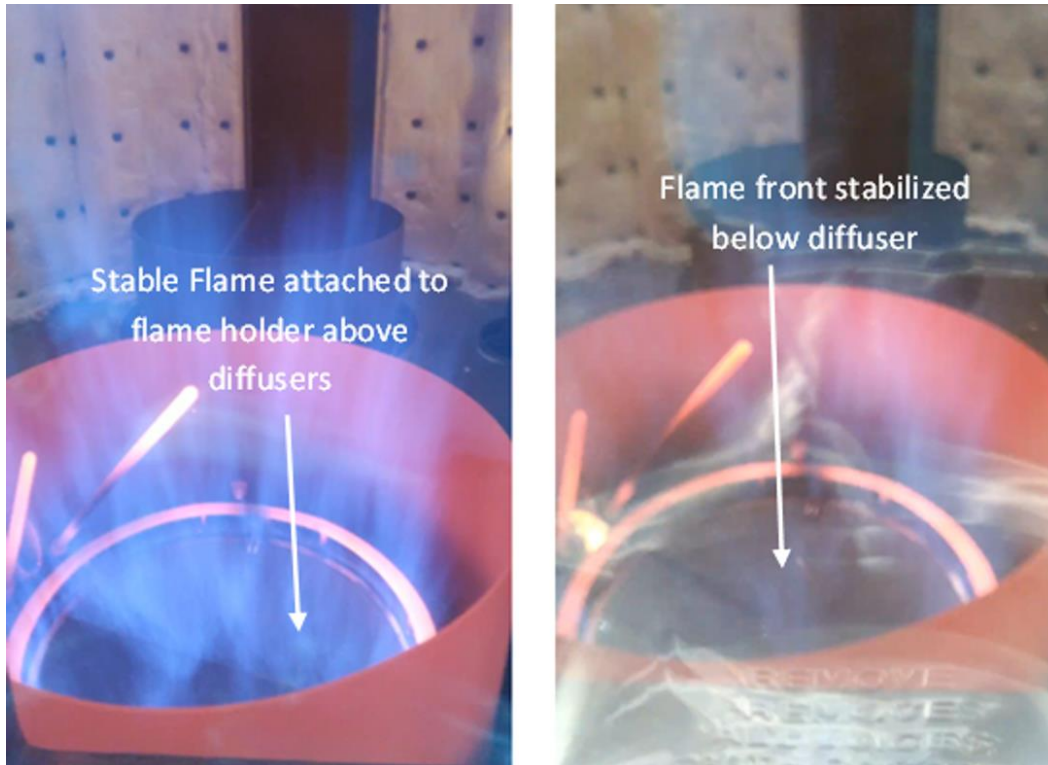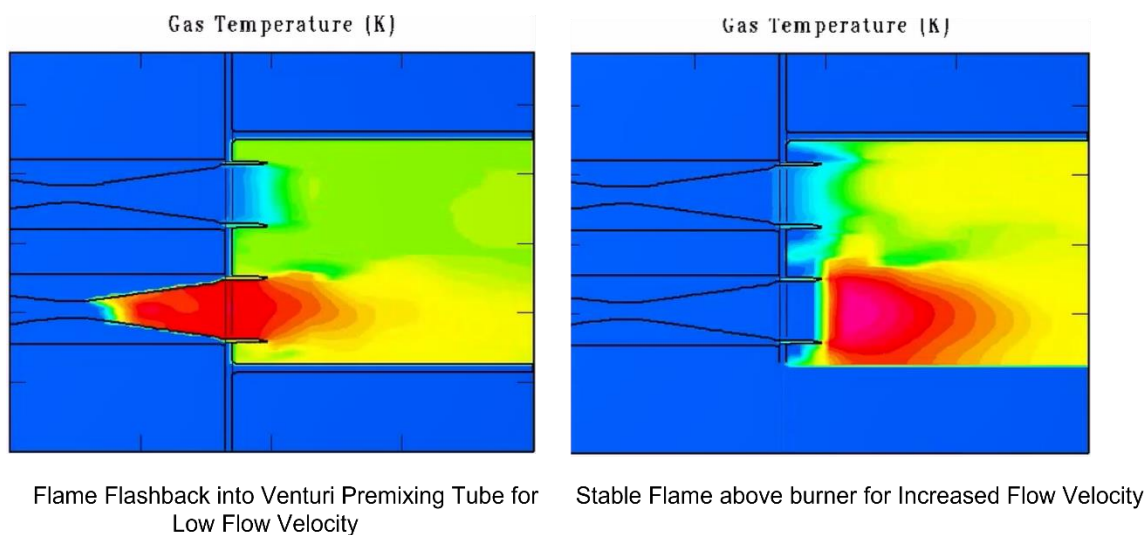

Figure 4 - Flame transition to unstable combustion observed during field tests

Flame Flashback into Venturi Premixing Tube for Low Flow Velocity   Stable Flame above burner for Increased Flow Velocity

Figure 5 - Unstable combustion simulation showing flame stabilization below burner diffuser with recirculation zone forming in combustion chamber

Flame Tube Length Optimization

The original premixed burner design used an 18" tall flame tube above which the flame is intended to stabilize. During our flash back analysis, the flame tube length was also examined. As shown in Figure 6, the length of the flame tube appears to affect the radial flame profile. For a 9" flame tube, the flame appears to be deformed near the center of the burner face. This observation would be more critical for burner designs with larger diameters. Since the current burner was larger than normally used in this enclosed flare design, it was thought that flame tube was also contributing to flame instability. Therefore, two additional CFD analyses were completed to examine flame tube length. As shown, the 6" tall flame tube appeared to provide a flatter radial flame profile above the burner compared to the 9 or 18" flame tubes. A 4" tall flame tube was also considered, and it appeared to provide a marginally flatter radial flame profile. But the respective improvement over the 6" flame tube was marginal. Also, moving the flame stabilization point closer to the burner face would increase the burner surface temperature so the best design was selected as the 6" tall flame tube. This change was also implemented in the revised burner design.
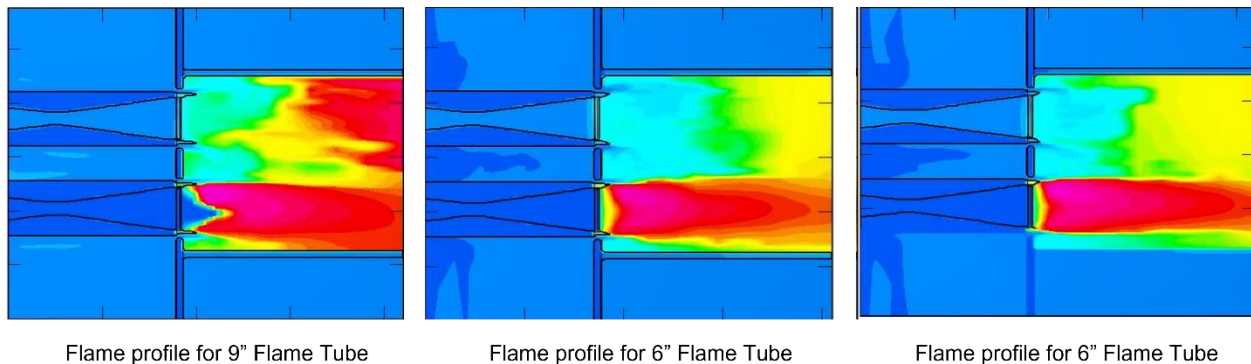

Flame profile for 9" Flame Tube   Flame profile for 6" Flame Tube   Flame profile for 6" Flame Tube
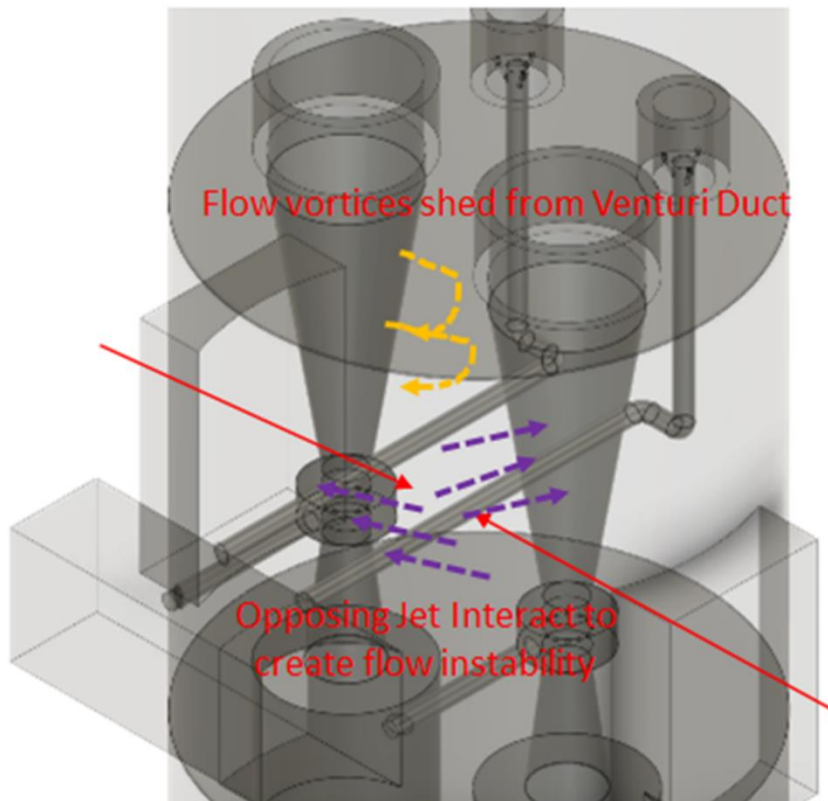
Figure 6 - Flame Tube Height CFD results

Burner Register Design

The last operational issue considered was related to the low-flow diffusion burner stability. During commissioning, the continuous pilot and low flow burner were blown out during high flow operation. Since the flare requires the low-flow burner and continuous pilot to remain operating during all flow conditions, this event required that it be investigated.

Initially, it was thought the diffusion flame was blown out by high flow velocity that greatly exceeded the respective flame speed. However, given results from the flash back study, this hypothesis was discarded because the flame flashed back at similar flow conditions in the premixed flame where local oxidizer is controlled prior to the flame. Since a diffusion flame
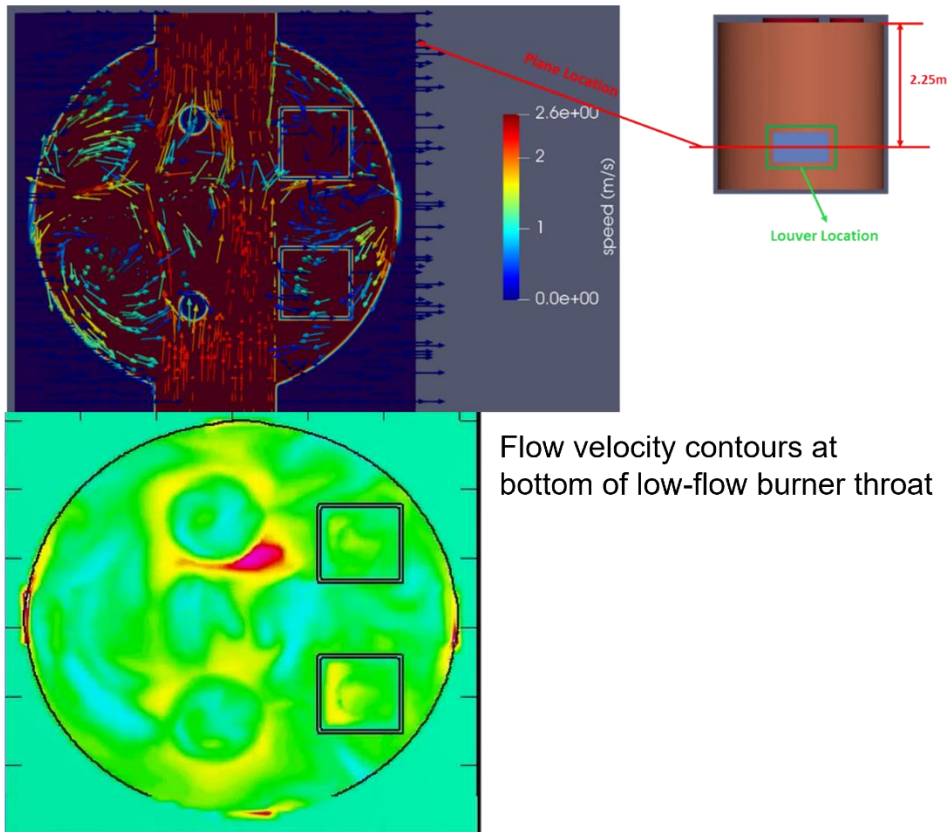
entrains the required air for complete combustion it is much more stable. For these reasons, this explanation for "flame-out" was deemed incorrect.

Observations of the low-flow burner flame during high firing conditions showed a flame that oscillated wildly just before "flame-out" was observed. This indicated flow instability in the combustion air fed to the low-flow burners. Examining design details showed that all combustion air came from below the burner deck as shown in Figure 7. The impact of unsteady combustion air flow in a burner plenum below a natural draft burner had previously been observed for a large process heater which included natural draft burners [21]. In this previous work, combustion above the burner relied on combustion air flowing from the combustion air plenum through burner registers up through the burner throat. The successful solution to this problem involved minimizing flow instabilities in the air plenum. Based on this experience, a detailed transient CFD analysis was done to simulate air flow into the flare below the burner deck. This flow was supplied through combustion air louvers located directly opposite each other in the flare. Air flowing through the louvers passed through the plenum up through the low-flow burner throat where it mixed with fuel fired through these burners. The predicted flow profile below the burner deck showed flow recirculation zones next to the burner throats (see Figure 8). This result suggested that burner registers be designed, built and installed below the low-flow burner inlets (see Figure 9). These registers were designed to moderate flow rates through the low-flow burner throat to eliminate large flame oscillations.

Figure 7 – Geometry below burner deck showing openings for combustion air supply to LF burners and relative orientation of louvers and pre-mixed burner ducts

Figure 8 – Flow instabilities below burner deck when Cold HF burner firing at 20 MMBtu/hr and LF Warm burner firing at 6 MMBtu/hr (note vortex shedding from venturi duct and interaction between inlet air from directly opposing louvers

Figure 9 – Placement of burner registers below the low-flow burner inlets

After these registers were installed, a CFD analysis showed flow profiles below the low-flow burners was much more uniform resulting in less flame instability (see Figure 10).

Velocity vectors near bottom of burner

Flow velocity contours at
bottom of low-flow burner throat

Figure 10 - Velocity vectors (top) and velocity contour immediately below low-flow burner inlet (bottom) show reduced flow instabilities below the low-flow burner inlets which reduced flame instabilities

CONCLUSIONS

During initial field testing of the enclosed flare, several issues were observed that were analyzed with the transient LES based CFD code C3d. Based on the analysis, the flare design was modified to improve flare performance. In addition, several firing conditions that characterized normal flare operation were analyzed with CFD. Results of this work helped ensure long term operation of the flare. After design modifications were made to the flare, subsequent testing verified each design change worked as predicted by CFD.

The revised enclosed flare has been fully commissioned and is working as required to support the plant which uses this flare to operate safely and efficiently.

REFERENCES

[1] C. Sondhauss, "About the Sound Vibrations of the Air in Heated Glass Tubes and in Covered Pipes of Unequal Width," *Ann Phy,* vol. 79, p. 1, 1850.

[2] G. Kelsall and C. Troger, "Prediction and Control of Combustion Instabilities in Industrial Gas Turbines," *Appl. Therm. Eng,* vol. 24, p. 1571–1582, 2004.

[3] A. Morgans and S. Stow, "Model-based Control of Combustion Instabilities in Annular Combustors," *Combust. Flame,* vol. 150, p. 380–399, 2007.

[4] C. Lawn and G. Penelet, "Common Features in the Thermoacoustics of Flames and Engines," *Int. J. of Spray and Comb Dyna,* vol. 10, no. 1, pp. 3-37, 2018.

[5] S. Hubbard and A. Dowling, "Acoustic Resonances of an Industrial Gas Turbine Combustion System," *ASME J. Eng. Gas Turb. Power,* vol. 123, p. 766–773, 2001.

[6] C. Pankiewitz and T. Sattelmayer, "Time Domain Simulation of Combustion Instabilities in Annular Combustors," *ASME J. Eng. Gas Turb. Power,* vol. 125, pp. 677-683, 2003.

[7] S. Roux, G. Lartigue, T. Poinsot, U. Meier and C. Bérat, "Studies of mean and unsteady flow in a swirled combustor using experiments, acoustic analysis, and large eddy simulations," *Combust. Flame,* vol. 141, pp. 40-54, 2005.

[8] M. Greiner and A. Suo-Anttila, "Validation of the ISIS Computer Code for Simulating Large Pool Fires Under a Varity of Wind Conditions,," *ASME J. Pressure Vessel Technology,* vol. 126, pp. 360-368, 2004.

[9] J. Smith, A. Suo-Anttila, N. Philpott and S. Smith, "Prediction and Measurement of Multi-Tip Flare Ignition," Sheraton Maui, Hawaii - SepteSheraton Maui, Hawaii, September 26 –29 (2010).

[10] J. Smith, R. Jackson, V. Sreedharan, A. Suo-Anttila, Z. Smith, D. Allen, D. DeShazer and S. Smith, "Safe Operation of Adjacent Multi-Point Ground Flares: Predicted and Measured Flame Radiation in Cross Flow Wind Conditions," Sheraton Kauai Resort, Kauai, Hawaii, September 9 –11 (2016).

[11] J. Smith, Jackson, R.E., Z. Smith, D. Allen and S. Smith, "Transient Ignition of Multi-Tip Ground Flares," in *American Flame Researach Committee Meeting*, University of Utah, Salt Lake City, Utah, September 17- 19 (2018).

[12] A. Suo-Anttila, K. Wagner and M. Greiner, "Analysis of Enclosure Fires Using the ISIS-3D CFD Engineering Analysis Code," in *Proceedings of ICONE12, 12th International Conference on Nuclear Engineering*, Arlington, Virginia, April 25-29, 2004.

[13] M. Greiner and A. Suo-Anttila, "Validation of the ISIS Computer Code for Simulating Large Pool Fires Under a Varity of Wind Conditions," *ASME J. Pressure Vessel Technology,* vol. 126, pp. 360-368, 2004.

[14] J. Smith, A. Suo-Anttila, S. Smith and J. Modi, "Evaluation of the Air-Demand, Flame Height, and Radiation Load on the Wind Fence of a Low-Profile Flare Using ISIS-3D,"," in *AFRC-JFRC 2007 Joint International Combustion Symposium*, Marriott Waikoloa Beach Resort, Hawaii, October 21-24, (2007).

[15] J. Smith, R. Jackson, V. Sreedharan, Z. Smith and A. Suo-Antilla, "Lessons Learned from Transient Analysis of Combustion Equipment in the Process Industries," in *AFRC 2019 - AFRC Industrial Combustion Symposium*, Hilton Waikoloa Village, Hawaii, September 9-11, 2019.

[16] J. Smith, A. Suo-Anttila, V. Sreedharan and Z. Smith, "Simulation of the Thermal-Acoustic Coupling Inside an Industrial Hazardous Waste Incinerator," in *AFRC 2020 Industrial Combustion Symposium*, Houston, Texas (online), October 19-20, 2020.

[17] R. Said, A. Garo and R. Borghi, "Soot Formation Modeling for Turbulent Flames," *Combustion and Flame,* vol. 108, pp. 71-86, 1997.

[18] B. Magnussen and B. Hjertager, "On Mathematical Models of Turbulent Combustion with Special Emphasis on Soot Formation and Combustion," *Sixteenth Symposium (International) on Combustion,* pp. 719-729, 1976.

[19] A. J. Suo-Anttila, "C3d Combustion Model Validation," Albuquerque, January 2019.

[20] C. Westbrook and F. Dryer, "Cheimcal Kinetic Modeling of Hydrocarbon Combustion," *Combust. Sci.,* vol. 10, pp. 1-57, 1984.

[21] J. Smith, M. Henneke, C. Schnepper and M. Lorra, "Application of Computational Fluid Dynamics to Industrial Opportunities at the John Zink Company," in *Chemical Reaction Engineering VII: Computational Fluid Dynamics*, Quebec, Canada, August 6-11, 2002.

[22] J. Smith, R. Jackson, V. Sreedharan, Z. Smith and A. Suo-Antilla, "Lessons Learned from Transient Analysis of Combustion Equipment in the Process Industries," in *AFRC 2019 - Industrial Combustion Symposium*, Hilton Waikoloa Village, Hawaii, September 9-11, 2019.

[23] J. Smith, A. Suo-Anttila, S. Smith and J. Modi, "Evaluation of the Air-Demand, Flame Height, and Radiation Load on the Wind Fence of a Low-Profile Flare Using ISIS-3D," in *AFRC-JFRC 2007 Joint International Combustion Symposium*, Marriott Waikoloa Beach Resort, Hawaii, October 21-24, 2007.

[24] J. Smith, Jackson, R.E., Z. Smith, D. Allen and S. Smith, "Transient Ignition of Multi-Tip Ground Flares," University of Utah, Salt Lake City, Utah, September 17- 19 (2018).

[25] A. Suo-Anttila and J. Smith, "Application of ISIS Computer Code to Gas Flares Under Varying Wind Conditions," in *2006 American Flame Research Committee International Symposium*, Houston, Texas, October 16-18, 2006.